# Developing a framework for studying brain networks in neonatal hypoxic-ischemic encephalopathy

Finn Lennartsson[1,2], Angela Darekar[3], Koushik Maharatna[4], Daniel Konn[5], David Allen[5], J-Donald Tournier[6,7], John Broulidakis[1], Brigitte Vollmer[1]

[1]Clinical Neurosciences, Clinical and Experimental Sciences, Faculty of Medicine, University of Southampton; Paediatric Neurology, Southampton Children's Hospital, Southampton, UK
[2]Department of Clinical Sciences Lund, Diagnostic Radiology, Lund University, Lund, Sweden
[3]Department of Medical Physics, University Hospital Southampton NHS Foundation Trust, Southampton, UK
[4]Electronics and Computer Science, University of Southampton, UK
[5]Clinical Neurophysiology, University Hospital Southampton NHS Foundation Trust, Southampton, UK
[6]Department of Biomedical Engineering, School of Bioengineering and Imaging Sciences, King's College London, London, UK
[7]Centre for the Developing Brain, School of Bioengineering and Imaging Sciences, King's College London, London, UK
finn.lennartsson@med.lu.se

**Abstract.** Newborns with hypoxic-ischemic encephalopathy (HIE) are at high risk of brain injury, with subsequent developmental problems including severe neuromotor, cognitive and behavioral impairment. Neural correlates of cognitive and behavioral impairment in neonatal HIE, in particular in infants who survive without severe neuromotor impairment, are poorly understood. It is reasonable to hypothesize that in HIE both structural and functional brain networks are altered, and that this might be the neural correlate of impaired cognitive and/or behavioral impairment in HIE.

Here, an analysis pipeline to study the structural and functional brain networks from neonatal MRI in newborns with HIE is presented. The structural connectivity is generated from dense whole-brain tractograms derived from diffusion-weighted MR fibre tractography. This investigation of functional connectivity focuses on the emerging resting state networks (RSNs), which are sensitive to injuries from hypoxic-ischemic insults to the newborn brain. In conjunction with the structural connectivity, alterations to the structuro-functional connectivity of the RSNs can be studied. Preliminary results from a proof-of-concept study in a small cohort of newborns with HIE are promising. The obstacles encountered and improvements to the pipeline are discussed. The framework can be further extended for joint analysis with EEG functional-connectivity.

**Keywords:** hypoxic-ischemic encephalopathy, connectivity, diffusion MRI, resting-state functional MRI, networks, human brain

# 1    Introduction

Neonatal hypoxic-ischaemic encephalopathy (HIE) as a consequence of perinatal asphyxia is associated with a high risk for brain injury and subsequent neurological and cognitive impairment[1]. Early diagnosis and outcome prediction is important to facilitate early intervention, enhance management and improve outcomes. Therapeutic hypothermia (TH), a neuroprotective intervention, reduces mortality and severe motor symptoms (cerebral palsy, CP) in toddlers with a history of neonatal HIE[2] . However, even after TH, cognitive impairments are frequent (up to 60%) in children with HIE, even in the absence of severe neuromotor impairment[3].

Neonatal Magnetic Resonance Imaging (MRI) is performed routinely after TH, with the aim of assessing the severity of brain injury and aiding prediction of neurodevelopmental outcome, However, the neural correlates of cognitive and behavioural impairment in neonatal HIE are poorly understood, particularly in the large proportion of infants who survive without  CP. Recent animal work[4] suggests that neonatal HI disrupts large scale functional pathways between the prefrontal cortex and hippocampus, which are linked to cognition. This occurs even with minor/moderate morphological brain changes, and network alterations persist beyond neonatal age[4].

A few studies have examined injuries on the developing brain networks in humans, showing alterations of networks' structures in prematurity and intrauterine growth restriction which correlate with cognitive development in toddlers[5, 6]. The effects of HIE on early development of brain networks has only been studied in 6-months old infants[7], and showed a trend of declining structural network integration and segregation with increasing neuromotor deficit[7]. However, there is currently no information in humans on how structural and/or functional connectivity alterations relate to cognitive outcome in the early years following neonatal HIE.

The aim of the current paper is to describe a framework for studying the structural and functional brain networks in newborns with HIE using MRI. As an extension of this framework, it also provides means for amalgamation with EEG functional-connectivity for combined analysis.

# 2    Methodological outline

Over the last few years, significant progress has been made in neuroimaging and neurophysiology with regard to characterizing the developing neural networks[8] and network alterations in neurodevelopmental disorders[9]. The structural connectome, i.e. the anatomical cortico-cortical and cortico-subcortical connections, can be reconstructed with diffusion-weighted MRI (dMRI) and fibre tractography. Anatomically separated brain regions also display so-called functional connectivity – they are co-activated during task-performance and during rest. Resting-state networks (RSN), studied using resting-state functional MRI (rs-fMRI), include spatially distinct networks activated in parallel during rest. To robustly characterize typical brain maturation and response to injury, one must consider structural and functional brain connectivity together. The emerging RSNs in the newborn brain are sensitive to injury from

HIE, and it is reasonable to hypothesize that alterations to the structural and functional connectivity of the RSNs, assessed in the neonatal period, are predictive of future cognitive outcome.

This paper describes a framework for studying the functional and structural connectomes using advanced MRI protocols and evaluation pipelines in the context of, but not only limited to, newborns with HIE. MRI of the newborn brain offers several challenges. Movement artifacts are common. The small brain size means that the relative sizes of the individual brain structures are also small, limiting their effective resolution. The yet unmyelinated white matter (WM) and the brain tissue's overall increased water content make the MR signal properties different from the mature brain. Therefore, specifically adapted neonatal MRI protocols and processing pipelines are required, and will be described in some detail in the following paragraphs.

## 3 Methods Part I: Processing of MRI data

### 3.1 Data acquisition

Neonatal MRI was performed on day 4-11 in newborns with HIE, allowing at least one day of re-warming after finishing the 72-hrs therapeutic hypothermia (TH). Infants were scanned during natural sleep, using the "feed-and-wrap" technique in which the baby is fed prior to imaging. The infant usually falls fast asleep and no sedation is required for imaging; this is a routine clinical procedure.

MRI was performed on a 3 Tesla MR scanner (Siemens Skyra VE11, Siemens AG, Erlangen, Germany), at Southampton General Hospital, UK. Participants were 13 newborns with moderate/severe HIE and undergoing TH at Princess Anne Hospital, Southampton, UK.

The routine clinical MRI protocol for infants with HIE consists of axial T1-weighted (T1w), proton density, T2-weighted (T2w), 3D-T1w (voxel size 0.8 mm x 0.8 mm x 0.8 mm), susceptibility weighted imaging (SWI) and diffusion-weighted MRI (dMRI), sagittal T2w and coronal T2w. Three sequences that were used for the work described in this paper were added to this routine protocol; a 3D-T2w (voxel size 0.9 mm x 0.9 mm x 0.9 mm), an rs-fMRI acquisition (voxel size 2.3 mm x 2.3 mm x 2.3 mm, full-brain coverage, 190 volumes with a TR=2.5 s, with an additional field map) and dMRI (voxel size 2.3 mm x 2.3 mm x 2.3 mm, full-brain coverage, multi-shell acquisition with 7 b=0, 16 b=400 s/mm$^2$, 58 b=2600 s/mm$^2$, and an additional 2 "b=0" volumes with reversed phase encode direction).

Ethics approval for use of anonymized data collected in the clinical context of the neurodevelopmental follow-up programme was granted by the University of Southampton, UK, Faculty of Medicine Ethics Committee (ID:26356).

### 3.2 Processing of structural MRI

The structural MRI (sMRI), consisting of the 3D-T1w and 3D-T2w images, captures the anatomical structures in the brain. Processing of sMRI involved four main

steps: brain extraction, image registration, brain tissue segmentation, and anatomical parcellation. The newborn brain has high water content and is still, largely, unmyelinated. Consequently, the T1w and T2w images have a different tissue contrast compared to adult images. Since most processing algorithms are developed for adult-like tissue contrasts, they require adaptation to neonatal images. Therefore, each of the four steps in the processing of sMRI will be explained in some details.

### 3.2.1    Brain extraction

Brain extraction of the neonatal sMRI often proves problematic when using the standard approaches developed for adult images, e.g. the FMRIB Software Library (FSL) brain extraction algorithm BET[10]. This was also the case with our acquired data. A pragmatic work-around was to use BET on the SWI magnitude images, which demonstrated good whole brain delineation, then co-register the SWI images to other image spaces (i.e. 3D-T1/T2w, dMRI and rs-fMRI spaces), and map the brain mask into these spaces. This approach gave very good results, but requires an SWI acquisition.

### 3.2.2    Image registration

Intra-subject registrations of the sMRI, dMRI and rs-fMRI datasets were carried out via linear/affine registration using FSL's FLIRT[11]. For improved registration of each participant's rs-fMRI to the sMRI data, a field map sequence was acquired in the research protocol. However, the field map could not, as of yet, be used for the neonatal registration pipeline with MIRTK (see below).

Inter-subject image registration is performed using a common template. However, few neonatal templates are publically available. The ALBERTs template (http://brain-development.org/brain-atlases/neonatal-brain-atlas-albert) was chosen for this study. Due to the different signal characteristics of the neonatal brain to the adult brain, adult registration algorithms have to be adapted for the neonatal registration or, alternatively, specific neonatal registration algorithms have to be used. This study opted for the MIRTK package (https://github.com/MIRTK), which has been extensively used for registration and segmentation of neonatal sMRI.

### 3.2.3    Brain tissue segmentation

Tissue segmentation of the neonatal brain is a challenging task because of the ongoing brain development and concurrent changes in MR signal characteristics. Manual segmentation can be performed but requires expertise and is very time-consuming. Automatic and/or semi-automatic techniques are preferred. This is an active area of research and several algorithms/techniques have been proposed/are being developed[12]. Commonly, segmentation algorithms primarily use the 3D-T2w images for segmentation since they have superior grey matter/white matter (GM/WM) contrast compared to the T1w images in the newborn. Multimodal techniques, e.g. combining

3D-T2w and 3D-T1w images, are being developed and show promising result but are, in general, not publically available[12, 13].

This project opted for the neonatal segmentation tool DrawEM (https://github.com/MIRTK/DrawEM)[14], which is part of MIRTK. DrawEM is an intensity-based technique utilizing the 3D-T2w images to automatically segment the neonatal brain into 87 regions, classified into GM, WM and cerebro-spinal fluid (CSF) and non-brain tissues classes, and corresponding to a parcellation of the brain into 50 anatomical regions[15]. It also outputs a tissue type classification, where every voxel is classified according to 9 tissue types as: CSF, cortical GM, WM, background, ventricles, cerebellum, deep GM, brainstem or hippocampi and amygdala. The DrawEM algorithm provided satisfactory results in the cohort for segmenting the cortical GM, but not the central brain structures. This is expected as unmyelinated WM is difficult to automatically segment in the neonate[12] and, consequently, the central brain structures (e.g. basal ganglia) do not display enough contrast on the T2w images for anatomical separation. However, reliable delineations of these structures are important in the fibre tractography. Therefore, the DrawEM segmentations had to be manually adjusted/edited. This was performed by an experienced neuroradiologist (FL).

The tissue type classification is used in the fibre tractography as an input to the ACT framework[16]. ACT uses the 5 tissue-type (5TT) format, in which the tissue is classified 5 tissue type classes: cortical or deep GM, WM, CSF or pathological tissue. The DrawEM tissue type classification could easily be mapped into the 5TT format using MRtrix command "labelconvert".

Illustrations of the DrawEM tissue segmentation and tissue type classification along with the manual editing are given in Fig. 1.
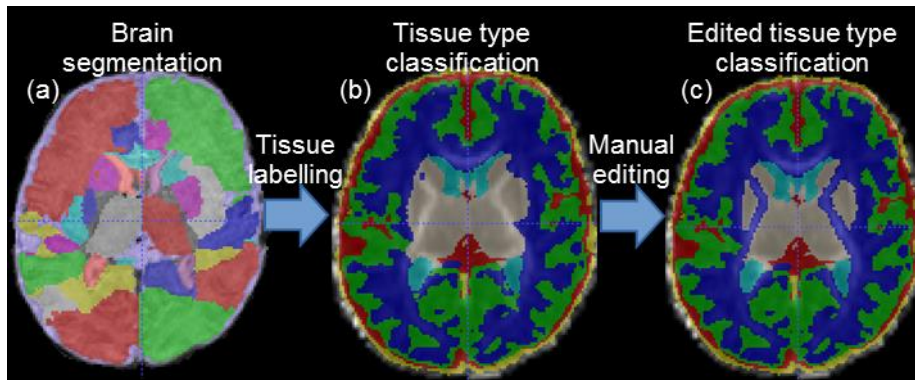


**Fig. 1** Segmentation of the 3D-T2w images with the DrawEM algorithm[14] (a). Notice the poor/absent definition of the anterior/posterior limbs of the internal capsule. Classification of the segmentation into 9 tissue types overlaid on a high-resolution FA-image (b), and the improvement after manual editing, especially of the central WM (c).

### 3.3    Processing of diffusion-weighted MRI

The diffusion-weighted MRI (dMRI) protocol (see above) was optimized for high-angular resolution diffusion imaging (HARDI), for improved separation of multiple white matter fibre populations in every voxel in the neonatal brain. The analysis pipeline was specifically developed for quantitative structural connectivity analysis of the fibre orientation distributions (FODs), estimated using a constrained spherical deconvolution (CSD)[17] approach within the software package MRtrix (J-D Tournier, Brain Research Institute, Melbourne, Australia, https://github.com/MRtrix3/mrtrix3). Changes in the dMRI signal, particularly the intra-cellular component at higher b-values, are translated into changes in the corresponding FOD amplitude of that fibre population. Spherical deconvolution can, thus, provide relevant parametric measures reflecting the underlying WM fibre structure[18].

Prior to any processing, visual inspection of all the raw dMRI data was carried out to detect excessive motion and/or signal dropouts. Thereafter, de-noising of raw dMRI data was performed[19], followed by estimation and correction of susceptibility and eddy-current induced distortions and motion-correction[20] using the reversed phase-encoding dataset.

For quantitative comparisons of FODs between brain voxels, it is important to adjust for slow signal variations from B1-inhomogeneities, to normalize the $b=0$ (no diffusion weighting) signal across subjects and to use a common response function. The first step is achieved using the popular N4-algorithm[21]. The normalization was done on a subject-specific basis by normalizing the $b=0$-images to the median of the $b=0$-value in a WM mask, where the mask was taken as the WM component in the 5TT image. This is not ideal as the WM may be influenced by pathology, some WM voxels are affected by partial volume effects from other tissue compartments and, presumably, the WM compartment may vary between subjects. An alternative, available in the latest release of MRtrix, is to normalize using the sum of all compartments in the multi-tissue CSD model. This is yet to be implemented in the current pipeline.

The response function is the dMRI signal expected for a voxel containing a single, coherently-oriented WM fibre bundle. Once estimated, the response function is used as the kernel in the spherical deconvolution step. This pipeline uses the "tournier" algorithm[22] for estimation of the response function in every subject, which are averaged to achieve a cohort-specific average response function. This, in turn, was used to estimate the FODs for all voxels in every subject using the high-shell dMRI data (i.e. b=2600 s/mm²) with CSD[17]. Estimation of diffusion tensors was also carried out using a weighted linear least squares estimation. From the diffusion tensors, parametric maps of fractional anisotropy (FA), as well as mean, axial (AD) and radial diffusivities (RD) and a color-coded FA-map were generated.

### 3.4    Processing of resting-state functional MRI

Resting-state functional MRI (rs-fMRI) can be used to detect the emerging resting-state networks (RSN) of the neonate[23, 24] to study the functional connectivity within and between the RSNs. Here, the aim was to use rs-fMRI to detect the RSNs in the

newborn with HIE, and to study RSN functional connectivity and its relation to the structural connectivity from dMRI. This study uses an exploratory approach by analyzing rs-fMRI data with (probabilistic) independent component analysis (ICA), implemented in FSL's Melodic[25].

Analysis of rs-fMRI in the newborn requires special methodological considerations[24]. Newborns examined during sleep typically exhibit occasional quirky movements which, by the nature of the ICA, may dominate the results. Excessive movement, absolute and/or relative, can be detected in the motion correction step of the fMRI time-series[11, 24]. Time-frames affected by excessive motion are commonly excised from the time-series before further analysis. This was implemented in the current study.

Deep sleep has been shown to change the connectivity strengths within RSNs in adults, but no such studies yet exists in newborns [23, 26]. However, studies in infants have shown of no large effect on the baseline BOLD signal from sleep, and several studies report no significant discrepancies in qualitative or quantitative results between infants scanned with and without sedation in rs-fMRI studies [23]. Moreover, the limited time of the imaging protocol may prevent the infant from falling into deep sleep, and minor variations in light sleep should not exert larger effects on the rs-fMRI analysis [26].

# 4 Methods Part II: Analysis of structural and functional brain connectivity

## 4.1 Structural connectivity

Probabilistic whole-brain fibre tractography was performed within the ACT-framework[16], using the 5TT maps generated from DrawEM tissue segmentation. A dense whole-brain tractogram of the order of $10^7$-$10^8$ streamlines was generated by seeding streamlines within the GM/WM interface from the 5TT map. The current $10^8$ whole-brain tractograms each took around 10 hrs to compute on a 16-core workstation. The tractogram was then filtered using the SIFT-method[27]. In SIFT, streamlines are iteratively removed from the tractogram until the streamline density within every voxel matches the integral of the underlying FOD lobe. This is based on the fact that the integral over an FOD lobe is proportional to the volume of the underlying dMRI tissue signal, particularly the intra-cellular component at higher b-values. In this way the total streamline count connecting any two regions in the tractogram can be viewed as a measure of the underlying connectivity of these two areas[27].
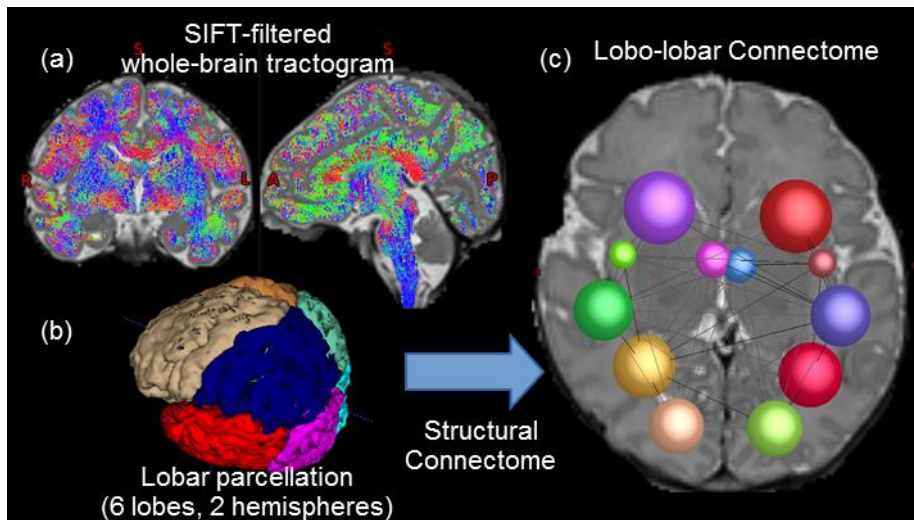
The SIFT-filtered tractograms were used to generate the structural connectome (the MRtrix command "tck2connectome"), with nodes as the anatomical brain regions given by the DrawEM tissue segmentation and edges as the set of streamlines connecting these regions. The structural connectome can be formulated as a connectivity matrix and can be analyzed by means of network analysis/graph theory analysis. Currently, the DrawEM brain segmentation includes 32 cortical cerebral regions. Other parcellation schemes, e.g. those including subcortical structures, could be considered,

but are currently not implemented within the DrawEM segmentation, mainly due the inability of the DrawEM algorithm to delineate the deep GM structures (see above), but should be explored. Examples of whole-brain tractograms and a structural connectome are given in Fig. 2.

## 4.2    Functional connectivity

The subject-level independent components (IC) were visually assessed to identify maps which were clearly of artifactual origin. These ICs were then regressed out of the rs-fMRI time-series. The "cleaned" rs-fMRI time-series were mapped into template space, by combining the registration between the fMRI time-series and 3D-T1w, and the 3D-T1w to T1-template (see above). An alternative approach is to use artifact-detection algorithms, such as FSL's FIX[28], but this requires training data which was not available in the pilot study.

The "cleaned" time-series were concatenated in the time domain, and group-level ICA (gICA) was performed. The ICs were inspected, and for every IC it was noted whether it belonged to a RSN or was artifactual. Dual regression estimations of activations in each individual, and network analysis was carried out using FSL's FSLNets (https://fsl.fmrib.ox.ac.uk/fsl/fslwiki/FSLNet) to show the interrelation between the different RSN. Results showed reliable identification of 11 ICs related to different RSNs in the cohort with adequate segregation of different RSNs (Fig. 3).



**Fig. 2.** The SIFT-filtered whole brain tractogram(a) is used together with a parcellation image (b) to generate the corresponding structural connectome(c). In this example the lobo-lobar connectome; the spheres depict the nodes (i.e. the cerebral lobes, including the insular cortices and the cingulate gyri), the edges depicts connections between nodes and the sphere sizes corresponds to the total streamline count (measure of connectivity).

### 4.3 Structural-functional connectivity

One of the aims was to carry out a joint analysis of the structural and functional connectivity within and between the RSNs. This would provide the structural-functional characteristics of emerging brain networks as quantitative measures to give precise information about structural and functional characteristics of the RSNs and specific networks of interest. This was done by looking at the structural connectivity between the cortical activation sites of the RSNs. The cortical components of the RSN activation, estimated from the gICA ICs using dual regression, were extracted using the DrawEM cortical segmentation. These then served as cortical targets to retrieve the streamlines in the SIFT-filtered whole-brain tractogram connecting these cortical areas. The structural connectivity between these activation sites could then be studied using the streamline count as a measure of connectivity. The approach for studying the structural-functional connectivity of the RSNs is shown in Fig. 4.
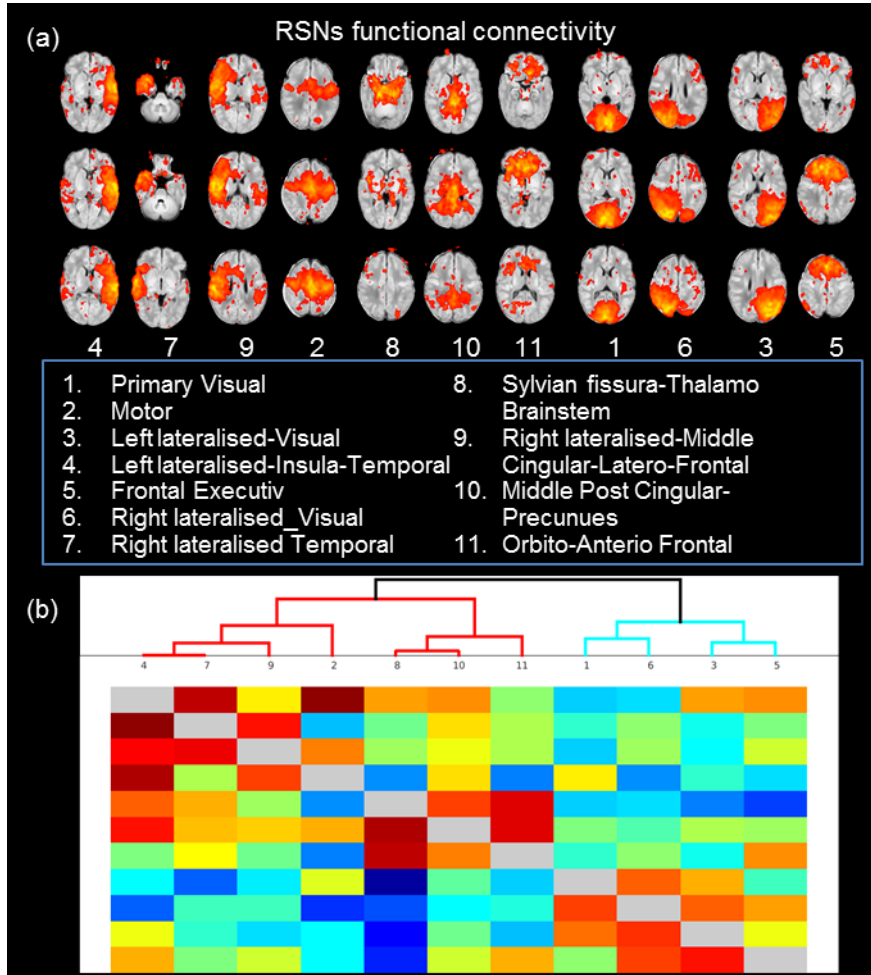
**Fig. 3.** The 11 RSNs identified in the cohort are visually assessed and classified (a). Dual regression is used to formulate a connectivity network matrix of connection strengths/correlations between the RSNs. This is analysed using basic network modelling in FSLNets (b), where red/green/blue represents strong/moderate/low connectivity between the numbered RSNs in (a). Notice the clustering of correlated RSNs into meaningful functional networks (e.g. RSNs 1-6-3-5 which are all related to visual processing), as well as the anti-correlation of others (b).

## 5  Discussion

This paper outlines a framework for studying the functional and structural connectivity in newborns with HIE using neonatal MRI. Achieving high quality, state-of-the-art image acquisition and processing for each of the sMRI, dMRI and rs-fMRI data sets, has been a great challenge within a clinical neonatal imaging setting. Nevertheless, in our pilot study of 13 newborns with HIE we could achieve good image quality

in about 80-90 % of cases. Some of the issues that arose and suggested solutions/improvements are suggested below.

## 5.1     MRI acquisition

MRI is challenging in newborns with HIE. In this pilot study, birth related bleeds were common, e.g. intra-cranial haemorrhages. These can cause image artifacts or hamper the image post-processing, e.g. the co-registration, unless they are masked out in the brain extraction. Motion during the scan was also frequent, mainly due to the baby waking up, and can be partly compensated for in the post-processing.

The imaging protocol can be further optimized, e.g. parameter optimization to improve GM/WM contrast in the sMRI to facilitate segmentation. If multiband acquisition were available on the MR scanner it should be used as this will reduce scan times substantially or increase efficiency, e.g. increase the number of time-points within the rs-fMRI acquisition by reducing the TR, and thus the time resolution.

## 5.2     Structural MRI

The segmentation of the sMRI can be improved. The subcortical parcellation with the current DrawEM algorithm is not accurate, mainly in areas of unmyelinated WM. This is important for fibre tractography, and the deep GM/WM structures had to be manually edited. Alternative registration and segmentations algorithms could be explored, e.g. using combined T1w and T2w contrasts [12]. The cortical GM showed occasional holes and could be remedied by a hole-filling algorithm. Finally, the anatomical parcellation map provided in DrawEM is limited to 50 anatomical brain regions and is not equally detailed across the brain (e.g. each temporal lobe contains 12 regions compared to one single region for the whole frontal lobe) [15]. More detailed parcellation schemes would be preferred[29]. As stated before, segmentation of the neonatal brain is challenging for various reasons [12]. However, there is a general need for more customized software and algorithms specifically targeting these issues, as most standard methods are only being tested in much older populations.

## 5.3     Diffusion MRI

The newborn brain is wet causing the dMRI signal to decay quickly, even at moderate b-values. This causes problems with the FOD estimation, especially in the deep periventricular frontal and parietal WM. As the SNR in dMRI signal decreases, the CSD estimation becomes noisy, which compromises the fibre tractography. Lowering the tracking cut-off values (FOD amplitude cut-off, down to 0.05 from 0.1) can ameliorate the problem but tractograms become noisier. Alternative response function estimators have been tested, e.g. the msmt_5tt framework[30]. However, in short, there is no simple answer to this and the current dMRI protocol is considered to give the best results.

## 5.4    Structuro-functional analysis

The structuro-functional analysis needs to be developed further. Currently, the structural connectivity can be studied for a single RSN (Fig. 4) and as the structural connectivity between the cortical activation sites for the RSN. However, HIE causes global injury affecting several RSNs, and their interactions. Therefore, a joint structure-functional analysis including all RSNs is desirable. The reconstruction of the structural connectome (using MRtrix command "tck2connectome") requires a parcellation input with non-overlapping regions. The cortical activation maps for all RSN do overlap (clearly seen in Fig. 3). The RSN activation maps could be thresholded to avoid anatomical overlap. An alternative would be to allow for activation overlap. This could be neuroanatomically reasonable as the limited dMRI resolution (voxel size 2 mm$^3$) cannot, even using HARDI, resolve distinct fiber populations along the "same" direction. For example, in the sub/juxtacortical WM, tracts "belonging" to separate RSNs would share FODs as they are reaching common cortical endpoints. However, along the majority of their paths they do not share FODs. Extracting the sets of streamlines from the SIFT-filtered whole-brain tractogram connecting the cortical activation maps of each RSN, and then formulating a common analysis would be a sensible approach, but the exact details of this would have to be considered further.
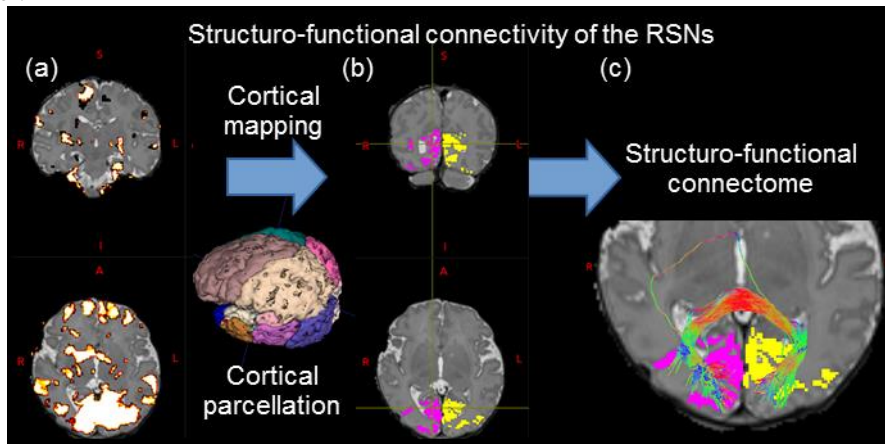


**Fig. 4** Subject-specific spatial maps of the RSNs (a) are mapped on the cortical surface (b) and together with the structural connectome, the structural connectivity within specific RSN can be studied (c). Here is an example of the interhemispheric connections within the primary visual RSN (IC 1).

## 5.5    Future directions

As suggested, several improvements can be made to the analysis pipeline. However, we have shown that is possible to study the structural and functional brain networks even in our small group of newborns with HIE. The small sample size of the pilot study limits association studies; further work on large samples is warranted.

One appealing future implementation would be to amalgate/extend the framework to a joint analysis with the functional connectivity derived from EEG. The structural and functional connectivity data can be used to improve the spatio-temporal characterization of the EEG-derived functional connectivity, e.g. by discrimination of direct and indirect connection. Moreover, for a more realistic coupling with the EEG source mapping, non-anatomically based parcellations can be considered [31].

Ultimately, our work aims at linking brain network metrics, metrics from EEG-derived connectivity, and clinical outcome data, which will be a promising new approach to improve early prediction of neurodevelopmental outcome and also early identification of those who will benefit from early intervention.

# 6    References

1. van Schie, P.E.M., Schijns, J., Becher, J.G., Barkhof, F., van Weissenbruch, M.M., Vermeulen, R.J.: Long-term motor and behavioral outcome after perinatal hypoxic-ischemic encephalopathy. Eur. J. Paediatr. Neurol. 19, 354–359 (2015).
2. Jacobs, S.E., Berg, M., Hunt, R., Tarnow-Mordi, W.O., Inder, T.E., Davis, P.G.: Cooling for newborns with hypoxic ischaemic encephalopathy. In: Cochrane Database of Systematic Reviews. John Wiley & Sons, Ltd (2013).
3. Schreglmann, M., Grund, A., Vollmer, B., Johnson, M.: Systematic Review: Long-term cognitive and behavioural outcome of neonatal hypoxic-ischaemic encephalopathy in children without CP. Arch. Dis. Child. Submitted (2018).
4. Domnick, N.-K., Gretenkord, S., De Feo, V., Sedlacik, J., Brockmann, M.D., Hanganu-Opatz, I.L.: Neonatal hypoxia–ischemia impairs juvenile recognition memory by disrupting the maturation of prefrontal–hippocampal networks. Exp. Neurol. 273, 202–214 (2015).
5. Batalle, D., Muñoz-Moreno, E., Tornador, C., Bargallo, N., Deco, G., Eixarch, E., Gratacos, E.: Altered resting-state whole-brain functional networks of neonates with intrauterine growth restriction. Cortex. 77, 119–131 (2016).
6. Batalle, D., Eixarch, E., Figueras, F., Muñoz-Moreno, E., Bargallo, N., Illa, M., Acosta-Rojas, R., Amat-Roldan, I., Gratacos, E.: Altered small-world topology of structural brain networks in infants with intrauterine growth restriction and its association with later neurodevelopmental outcome. NeuroImage. 60, 1352–1366 (2012).
7. Tymofiyeva, O., Hess, C.P., Ziv, E., Tian, N., Bonifacio, S.L., McQuillen, P.S., Ferriero, D.M., Barkovich, A.J., Xu, D.: Towards the "Baby Connectome": Mapping the Structural Connectivity of the Newborn Brain. PLOS ONE. 7, e31029 (2012).
8. Hagmann, P., Grant, P.E., Fair, D.A.: MR connectomics: a conceptual framework for studying the developing brain. Front. Syst. Neurosci. 6, 43 (2012).
9. Dennis, E.L., Thompson, P.M.: Reprint of: Mapping connectivity in the developing brain. Int. J. Dev. Neurosci. 32, 41–57 (2014).
10. Smith, S.M.: Fast robust automated brain extraction. Hum. Brain Mapp. 17, 143–155 (2002).

11. Jenkinson, M., Bannister, P., Brady, M., Smith, S.: Improved optimization for the robust and accurate linear registration and motion correction of brain images. NeuroImage. 17, 825–841 (2002).

12. Išgum, I., Benders, M.J.N.L., Avants, B., Cardoso, M.J., Counsell, S.J., Gomez, E.F., Gui, L., Hűppi, P.S., Kersbergen, K.J., Makropoulos, A., Melbourne, A., Moeskops, P., Mol, C.P., Kuklisova-Murgasova, M., Rueckert, D., Schnabel, J.A., Srhoj-Egekher, V., Wu, J., Wang, S., de Vries, L.S., Viergever, M.A.: Evaluation of automatic neonatal brain segmentation algorithms: The NeoBrainS12 challenge. Med. Image Anal. 20, 135–151 (2015).

13. Devi, C.N., Chandrasekharan, A., Sundararaman, V.K., Alex, Z.C.: Neonatal brain MRI segmentation: A review. Comput. Biol. Med. 64, 163–178 (2015).

14. Makropoulos, A., Gousias, I.S., Ledig, C., Aljabar, P., Serag, A., Hajnal, J.V., Edwards, A.D., Counsell, S.J., Rueckert, D.: Automatic Whole Brain MRI Segmentation of the Developing Neonatal Brain. IEEE Trans. Med. Imaging. 33, 1818–1831 (2014).

15. Gousias, I.S., Hammers, A., Counsell, S.J., Srinivasan, L., Rutherford, M.A., Heckemann, R.A., Hajnal, J.V., Rueckert, D., Edwards, A.D.: Magnetic Resonance Imaging of the Newborn Brain: Automatic Segmentation of Brain Images into 50 Anatomical Regions. PLoS ONE. 8, (2013).

16. Smith, R.E., Tournier, J.-D., Calamante, F., Connelly, A.: Anatomically-constrained tractography: Improved diffusion MRI streamlines tractography through effective use of anatomical information. NeuroImage. 62, 1924–1938 (2012).

17. Tournier, J.-D., Calamante, F., Connelly, A.: Robust determination of the fibre orientation distribution in diffusion MRI: non-negativity constrained super-resolved spherical deconvolution. NeuroImage. 35, 1459–1472 (2007).

18. Raffelt, D., Tournier, J.-D., Rose, S., Ridgway, G.R., Henderson, R., Crozier, S., Salvado, O., Connelly, A.: Apparent Fibre Density: a novel measure for the analysis of diffusion-weighted magnetic resonance images. NeuroImage. 59, 3976–3994 (2012).

19. Veraart, J., Novikov, D.S., Christiaens, D., Ades-aron, B., Sijbers, J., Fieremans, E.: Denoising of diffusion MRI using random matrix theory. NeuroImage. 142, 394–406 (2016).

20. Andersson, J.L.R., Graham, M.S., Zsoldos, E., Sotiropoulos, S.N.: Incorporating outlier detection and replacement into a non-parametric framework for movement and distortion correction of diffusion MR images. NeuroImage. 141, 556–572 (2016).

21. Tustison, N.J., Avants, B.B., Cook, P.A., Zheng, Y., Egan, A., Yushkevich, P.A., Gee, J.C.: N4ITK: Improved N3 Bias Correction. IEEE Trans. Med. Imaging. 29, 1310–1320 (2010).

22. Tournier, J.-D., Calamante, F., Connelly, A.: Determination of the appropriate b value and number of gradient directions for high-angular-resolution diffusion-weighted imaging. NMR Biomed. 26, 1775–1786 (2013).

23. Mongerson, C.R.L., Jennings, R.W., Borsook, D., Becerra, L., Bajic, D.: Resting-State Functional Connectivity in the Infant Brain: Methods, Pitfalls, and Potentiality. Front. Pediatr. 5, (2017).
24. Smyser, C.D., Neil, J.J.: Use of resting-state functional MRI to study brain development and injury in neonates. Semin. Perinatol. 39, 130–140 (2015).
25. Beckmann, C.F., Smith, S.M.: Probabilistic independent component analysis for functional magnetic resonance imaging. IEEE Trans. Med. Imaging. 23, 137–152 (2004).
26. Gao, W., Lin, W., Grewen, K., Gilmore, J.H.: Functional Connectivity of the Infant Human Brain: Plastic and Modifiable. Neurosci. Rev. J. Bringing Neurobiol. Neurol. Psychiatry. 23, 169–184 (2016).
27. Smith, R.E., Tournier, J.-D., Calamante, F., Connelly, A.: SIFT: Spherical-deconvolution informed filtering of tractograms. NeuroImage. 67, 298–312 (2013).
28. Salimi-Khorshidi, G., Douaud, G., Beckmann, C.F., Glasser, M.F., Griffanti, L., Smith, S.M.: Automatic denoising of functional MRI data: Combining independent component analysis and hierarchical fusion of classifiers. NeuroImage. 90, 449–468 (2014).
29. Blesa, M., Serag, A., Wilkinson, A.G., Anblagan, D., Telford, E.J., Pataky, R., Sparrow, S.A., Macnaught, G., Semple, S.I., Bastin, M.E., Boardman, J.P.: Parcellation of the Healthy Neonatal Brain into 107 Regions Using Atlas Propagation through Intermediate Time Points in Childhood. Brain Imaging Methods. 220 (2016).
30. Jeurissen, B., Tournier, J.-D., Dhollander, T., Connelly, A., Sijbers, J.: Multi-tissue constrained spherical deconvolution for improved analysis of multi-shell diffusion MRI data. NeuroImage. 103, 411–426 (2014).
31. Tymofiyeva, O., Ziv, E., Barkovich, A.J., Hess, C.P., Xu, D.: Brain without Anatomy: Construction and Comparison of Fully Network-Driven Structural MRI Connectomes. PLoS ONE. 9, e96196 (2014).